Asian Journal of Chemistry; *Vol. 33, No. 6 (2021), 1389-1395*

ASIAN JOURNAL OF CHEMISTRY

https://doi.org/10.14233/ajchem.2021.23194

Anti-Corrosive Behaviour of *Saccharum officinarum* Extract in 15% HCl for Stainless Steel-410 Surface

NISHANT BHARDWAJ[1], POOJA SHARMA[2] and VINEET KUMAR[2,*]

[1]Department of Chemistry, Lovely Professional University, Phagwara-144411, India
[2]Department of Biotechnology, Lovely Professional University, Phagwara-144411, India

*Corresponding author: E-mail: vineetkumar22@gmail.com

Received: 6 March 2021; *Accepted*: 23 April 2021; *Published online*: 5 June 2021; AJC-20373

The objective of this study is to experimentally evaluate the inhibition properties of *Saccharum officinarum* extract in a 15% hydrochloric acidic media for stainless steel (SS-410). The gravimetric, UV spectroscopy, FTIR and surface morphological studies carried out using SEM, AFM and XRD revealed that the *S. officinarum* extract protected the SS 410 steel in 15% hydrochloric acidic medium. Gravimetric analysis revealed maximum 95.92 % inhibition efficiency at 4 g/L inhibitor concentration. The computational studies (quantum chemical calculations) were further utilized to understand the concept of chelation mechanism. The surface film formation and other 3D features of *S. officinarum* extract film over SS-410 surface was confirmed using AFM studies. Adsorption of *S. officinarum* extract over SS-410 surface followed Langmuir adsorption isotherm. It is clear from the theoretical and computational studies that the *S. officinarum* extract acted as mixed type inhibitor by adsorption of hybrid organic-inorganic inhibitor ingredients on SS-410. Thus, *S. officinarum* extract can develop an efficient protective layer on SS-410 that has various industrial applications.

Keywords: *Saccharum officinarum* extract, Electrochemical impedance spectroscopy, Potentiodynamic polarization.

INTRODUCTION

Every year around 75,000 billion USD are lost due to corrosion. It accounts for 3.4% of world's GDP loss. In India, corrosion causes loss of 1670 billion USD which is equivalent to 4.2% of the total GDP [1]. Metal corrosion is one of the serious problems faced by many industries. Many studies are reported worldwide to find suitable solutions to this major issue [2]. Fe-Cr-C alloys has been are specially designed for those components which requires more mechanical strength and high to moderate resistance to corrosion. The 400 series of stainless steel is among those martensitic steels which are widely used in petroleum industries specifically in petroleum production and refining, turbine components, fasteners and machinery parts [3]. Various industrial processes namely acid pickling, acid cleaning and descaling, oil well acidization utilizes mineral acids. Hydrochloric acid and sulphuric acid are commonly used mineral acids [4,5]. Use of H_2SO_4 leads to formation of insoluble products. Therefore, petroleum industries mostly uses 15% HCl for descaling purpose as no insoluble products are left after the treatment. However, usage of HCl also has limitations as it adversely affects the metal surfaces of the machinery parts during the cleaning process leading to corrosion [6].

The destruction of metal components can be avoided by using corrosion inhibitors [7,8]. Most of the inhibitors try to prevent the dissolution of metals due to acid attack. Most of the inhibitors working in an acid aggressive environment contain organic compounds as key ingredients. These compounds contains nitrogen, oxygen and/or sulphur atoms, heterocyclic compounds and π-electrons. The inhibitors for acidic environment get absorbed on the surface of steel through physisorption or chemisorption or both and thus resist corrosion. Among various types of corrosion inhibitors, green corrosion inhibitors are preferred over chemical inhibitors. Extract based corrosion inhibitors are of specific interest. More specifically use of crop seed waste material is better option as indirectly it also reduce waste accumulation in environment and help farmer to have earning from waste [9-11].

Saccharum officinarum is a grass diverse genus with 25-30 species of deciduous flowering seeds in the family Poaceae.

After harvesting seeds, most of the vegetative residues are unutilized and pile up as waste. Also due to lack of strategies for the disposal of such wastes results for the environmental pollution. The main aim of this study is to investigate the use of *S. officinarum* as corrosion inhibitor.

EXPERIMENTAL

Working electrode and *S. officinarum* extract (SOE) preparation: For the preparation of working electrode, SS-410 specimens of 10 mm diameter were immersed in epoxy resin. The elemental composition of used stainless steel was Fe (87.2%), Cr (11.14%), Mn (0.82%), Cu (0.43%), C (0.134%), P (0.02%) and Si (0.005%). Working electrode surface was abraded by using emery paper of 100, 320, 600, 800, 1000 and 1200 grades. *S. officinarum* seed wastes were collected from agriculture land near Jalandhar city, India and identification was done by botanical survey of India, Dehradun. Seeds were dried for 2 days under sunshade and grinded to powder. The powdered sample, 100 g was extracted with 450 mL of methanol at 75 ºC for 72 h. The extracted solution was filtered and the pH of the aqueous solution was found to be 9. The filtered liquid was evaporated with the help of Soxhlet evaporator and allowed to dry completely in a vacuum desiccator. The obtained *S. officinarum* extract was dissolved in 15% HCl designated as corrosive medium in this study. The *S. officinarum* extract solutions of different concentrations *viz*. 1, 2, 3 and 4 g/L were prepared in 15% HCl corrosive medium.

Weight loss measurement: Weight loss tests were performed at 1-4 g/L *S. officinarum* extract in 15% HCl medium at room temperature for 24 h [12]. For the weight loss experiment SS-410 sample having the dimension, 5 cm × 5 cm × 0.3 cm was used. The SS-410 samples were weighed and immersed in the test solution in the absence and presence of *S. officinarum* extract for 24 h. After 24 h, the SS-410 samples were taken out from the test solution, rinsed with acetone, dried under nitrogen flow and weighed.

Electrochemical impedance spectroscopy: Auto lab electrochemical Workstation (Metrohm) with three-electrode electrochemical cell were used for electrochemical impedance and Tafel polarization measurements. The obtained Tafel polarization curves were recorded between -200 to +200 mV *versus* Ag/AgCl (3 M KCl) with scanning rate of 0.1 mV/s. The electrochemical measurements were conducted at 10 mV amplitude and 100 kHz to 0.01 Hz frequency. Obtained data were calculated by using CHI 760C electrochemical work station software.

FTIR: The FTIR spectra (FTIR 8400S spectrophotometer, Shimadzu) were recorded between 4000-500 cm^{-1} wavelength to identify the functional groups present over the phytochemicals in the *S. officinarum* extract. The spectra of the *S. officinarum* extract were recorded at different conditions before the immersion of SS-410 in 4 g/L concentration in 15% HCl.

UV-visible: The preliminary anticorrosion activity of *S. officinarum* extract prepared in 15% HCl solution were recorded using UV-Vis 1800 spectrophotometer (Shimadzu). The UV analysis were performed using two set of experiments. In the first set of conditions, the UV-visible spectra of 4 g/L the *S. officinarum* extract containing 15% HCl solution was recorded. In the second set, the spectrum was recorded for 15% HCl solution in absence of the *S. officinarum* extract.

Atomic force microscopic (AFM) study: INTEGRA AFM model (NT-MDT) was used for the surface investigation of SS-410. For the AFM study, the surface of stainless steel was cleaned using ultrapure water followed by acetone. Abraded steel, steel immersed in corrosive media and steel immersed in 15% HCl solution containing 4 g/L SOE were characterized using AFM.

SEM: Scanning electron microscope (SEM, JEOL) was used for taking the surface micrograph of steel. The SEM images were captured for polished steel and steel samples immersed in corrosive media in the absence and presence of 4 g/L *S. officinarum* extract.

XRD: The SS-410 strips were immersed in 15% HCl solution in absence and presence of 4 g/L *S. officinarum* extract. SS-410 samples were dried and used for XRD characterization. PHI 5000 Versa Probe III model (ZEOL) was used for XRD study.

Theoretical computation studies: Hyperchem (8.0) were used for theoretical studies of anti-corrosion activity of phytochemicals present in the *S. officinarum* extract. The studies were analysed using principle of density functional theory (DFT). The energies of frontier molecular orbitals were used as the main parameters in this study.

RESULTS AND DISCUSSION

Weight loss measurement: The corrosion inhibition efficiency of *S. officinarum* extract was calculated for the surface of SS-410 in the presence of corrosive 15% HCl medium. Corrosion rate of SS-410 in corrosive media using different concentration of SOE were calculated using eqn. 1:

$$C_R = \frac{K \times W}{A \times t \times \rho} \tag{1}$$

where, C_R is the notation of corrosion rate (mm $year^{-1}$), w is used for notation of weight loss of stainless steel, t belongs to the immersion time (h) of SS-410, ρ is the density (7.86 g cm^{-3}) of the steel as per the literature of ASTM G 31-72 and k is the notation of corrosion constant (8.76 × 10^4) [13].

The value of corrosion inhibition efficiency (IE) and the surface coverage (θ) of *S. officinarum* extract was calculated with the help of eqns. 2 and 3:

$$\text{IE } (\%) = \frac{C_R^o - C_R^i}{C_R^o} \times 100 \tag{2}$$

$$\theta = \frac{C_R^o - C_R^i}{C_R^o} \tag{3}$$

where, the corrosion rate of immersed SS-410 in corrosive media and in *S. officinarum* extract solution was mentioned by C_R^o and C_R^i, respectively. As the concentration of *S. officinarum* extract increases, the value of corrosion rate decreases thus leading to increase in corrosion inhibition efficiency. The decrease in the value of corrosion rate is due to adsorption of *S. officinarum* extract phytochemicals on the surface of SS-

410. Maximum 95.92 % corrosion inhibition efficiency was recorded using 4g/L *S. officinarum* extract. The values of the main parameters are mentioned in Table-1.

TABLE-1
PARAMETERS OF WEIGHT LOSS PARAMETERS FOR DIFFERENT CONCENTRATION OF HCl WITH SOE 24 h AT 298 K

Concentration	Corrosion rate, C_R (mmy^{-1})	Inhibition efficiency (%)	Surface coverage, θ	C/θ
15% HCl	39.01	–	–	–
15% HCl + 1 g/L SOE	26.784	31.34	0.3134	3.19
15% HCl + 2 g/L SOE	16.782	56.98	0.5698	3.51
15% HCl + 3 g/L SOE	9.233	76.33	0.7633	3.93
15% HCl + 4 g/L SOE	1.591	95.92	0.9592	4.17

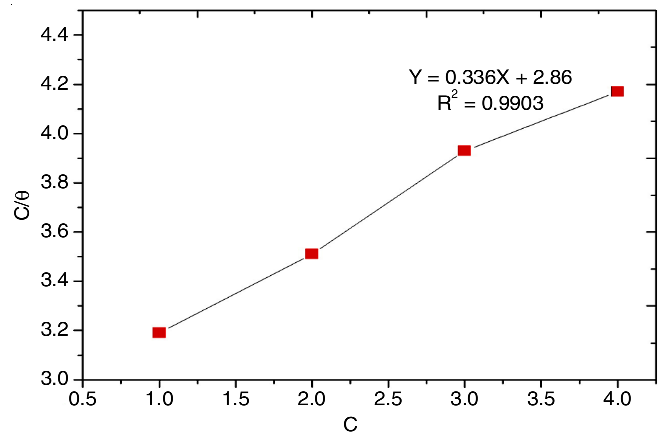

Fig. 1. Langmuir isotherm adsorption (C/θ vs. C) based on weight loss measurements of the *S. officinarum* extract (SOE) on SS-410 surface 15 % HCl for 24 h

Adsorption isotherm study: Langmuir adsorption isotherm (eqn. 4) was used to explain the adsorption behaviour of *S. officinarum* extract on SS-410 surface. The concentration and the value of surface coverage of *S. officinarum* extract provided to SS-410 were the main component of this study.

$$\frac{C}{\theta} = \frac{1}{K_{ads}} + C \qquad (4)$$

The linear correlation coefficient (0.9903) is almost equal to 1 (Fig. 1), which confirms that adsorption of *S. officinarum* extract obeys Langmuir adsorption isotherm [14].

Electrochemical study

Potentiodynamic polarization: The working electrode of SS-410 was immersed in 15% HCl solution with 1, 2, 3 and 4 g/L of *S. officinarum* extract solution. There was decrease in current densities with increase in *S. officinarum* extract concentration from 1 g/L to 4 g/L (Table-2). The value of corrosion inhibition efficiency was calculated using eqn. 5 [15].

$$IE\ (\%) = \frac{I^{o}_{corr} - I^{i}_{corr}}{I^{o}_{corr}} \times 100 \qquad (5)$$

TABLE-2
POLARIZATION PARAMETERS FOR S.S.-410 STEEL IN 15% HCl WITHOUT AND WITH DIFFERENT CONCENTRATIONS OF SOE EXTRACT AT 298 K

Corrosive solution conc.	Corrosion current density, I_{corr} ($A\ cm^{-2}$)	Inhibition efficiency, η (%)
15% HCl solution	0.0000540030	–
15% HCl solution + 1 g/L SOE	0.0000317052	41.29
15% HCl solution + 2 g/L SOE	0.0000241285	55.32
15% HCl solution + 3 g/L SOE	0.0000100014	81.48
15% HCl solution + 4 g/L SOE	0.0000052869	90.21

where I^{o}_{corr} and I^{i}_{corr} were used for corrosion current density of 15% HCl solution and *S. officinarum* extract inhibitor solution. The polarization curve is shown in Fig. 2a. As the concentration of *S. officinarum* extract increases in the corrosive media, the value of corrosion current density decreases, which designate the increase in corrosion inhibition efficiency [16,17]. So, *S. officinarum* extract has mixed type of inhibition behaviour. A corrosion inhibition efficiency 90.23% was recorded at the

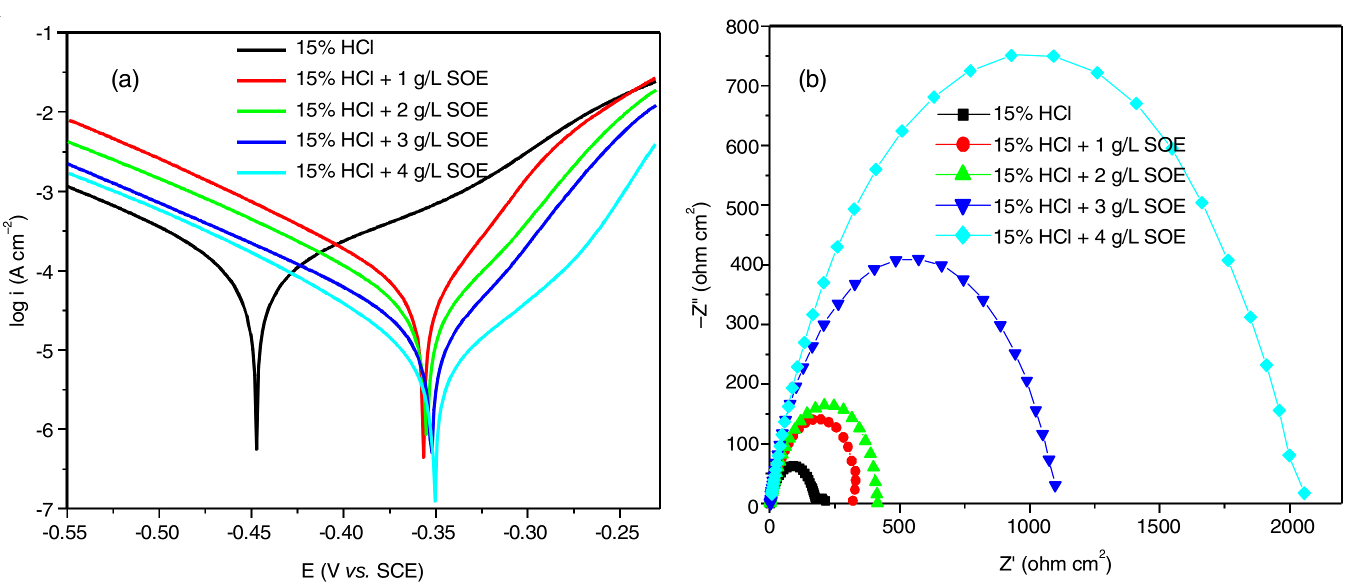

Fig. 2. (a) Tafel polarization curves for SS-410 in 15% HCl solution without and with different concentrations of *S. officinarum* extract (SOE) (b) Impedance data of SS-410 in 15% HCl solution with the concentration of 4 g/L *S. officinarum* extract (SOE) at 298 K

concentration of 4 g/L *S. officinarum* extract in 15% HCl solution.

Electrochemical impedance spectroscopy: Working electrode of SS-410 samples was immersed in 15% HCl solution having the different concentration of *S. officinarum* extract. In Fig. 2b, it can be seen that Nyquist plot contains a semi-circle in each curve which stands for a constant time, because of the charge transfer resistance. As the concentration of *S. officinarum* extract increases, the diameter of circle increases from 1 to 4g/L. This designates the increase in the corrosion inhibition efficiency. The corrosion inhibition efficiency were calculated using eqn. 6 [18]:

$$\text{IE (\%)} = \frac{R_{ct} - R^{o}_{ct}}{R_{ct}} \times 100 \quad (6)$$

where R_{ct} and R^{o}_{ct} designates the charge transfer resistance of different *S. officinarum* extract concentrations and 15% HCl solution, respectively. A maximum 91.23 % corrosion inhibition efficiency was obtained as shown in Table-3. A layer was formed, which proved from the R_{ct} value, as its values increases with increases the *S. officinarum* extract concentration [19]. The Bode plot has been shown in Fig. 3b. The *S. officinarum* extract get adsorbed on the surface of SS-410 by involving π-electrons of aromatic ring or the heteroatoms present in the phyto-chemicals to the vacant *d*-orbital of iron. The results obtained from EIS are in good agreement with the potentiodynamic polarization (PDP). The difference observed in the inhibition efficiency obtained from EIS and PDP may be due to the difference in the technique used. The PDP measurements provide real time kinetics of the electrochemical processes (polarization at wide range of potential with a possible irreversible change occur due to the measuring process) and EIS data are usually obtained at the open circuit potential (OCP) and provide measured values of the overall interfacial resistance at the electrode-electrolyte interface [20,21].

TABLE-3
EIS PARAMETERS FOR S.S.-410 STEEL IN 15% HCl WITHOUT AND WITH DIFFERENT CONCENTRATIONS OF SOE EXTRACT AT 298 K

Corrosive solution conc.	Charge transfer resistance, R_{ct} (Ω cm²)	Inhibition efficiency, η (%)
15% HCl solution	180.21	–
15% HCl solution + 1 g/L SOE	319.96	43.67
15% HCl solution + 2 g/L SOE	415.06	56.58
15% HCl solution + 3 g/L SOE	1115.89	83.85
15% HCl solution + 4 g/L SOE	2056.54	91.23

FTIR studies: Fig. 4 shows the FTIR spectra having the peaks of various functional groups. The peak at 3147.93 cm^{-1} shows the presence of O-H group and C=O stretching occurs at 1710.91 cm^{-1}. The vibration of aromatic ring present in extract shows peak at 1209.40 cm^{-1}. The FTIR also confirmed the presence of other functional groups. The *S. officinarum* extract shows that corrosion inhibition property is due to the presence of heteroatoms in the extract [22,23].

UV visible study: Fig. 5 shows the UV spectra of *S. officinarum* extract in 15% HCl before and after immersing the SS-410 specimen. In the case of before immersion, UV-visible peak of non SS-410 immersed was obtained having higher absorbance as compare to the after the corrosion test. In both the cases peaks representing π-π* and n-π* transition, were observed at 215 and 289 nm, respectively. But the UV visible peak intensity of *S. officinarum* extract in 15% HCl solution after SS-410 immersion was decreased compared to before SS-410 immersion sample. This decrease in peak intensity clearly demonstrates the adsorption of *S. officinarum* extract over SS-410 surface thus the free component decreases leading to decrease in peak intensity [26,27].

SEM study: The surface morphology of SS-410 in 15% HCl solution was also analyzed. In Fig. 6a-c, SEM images were captured for abraded steel, steel sample immersed in 15% HCl

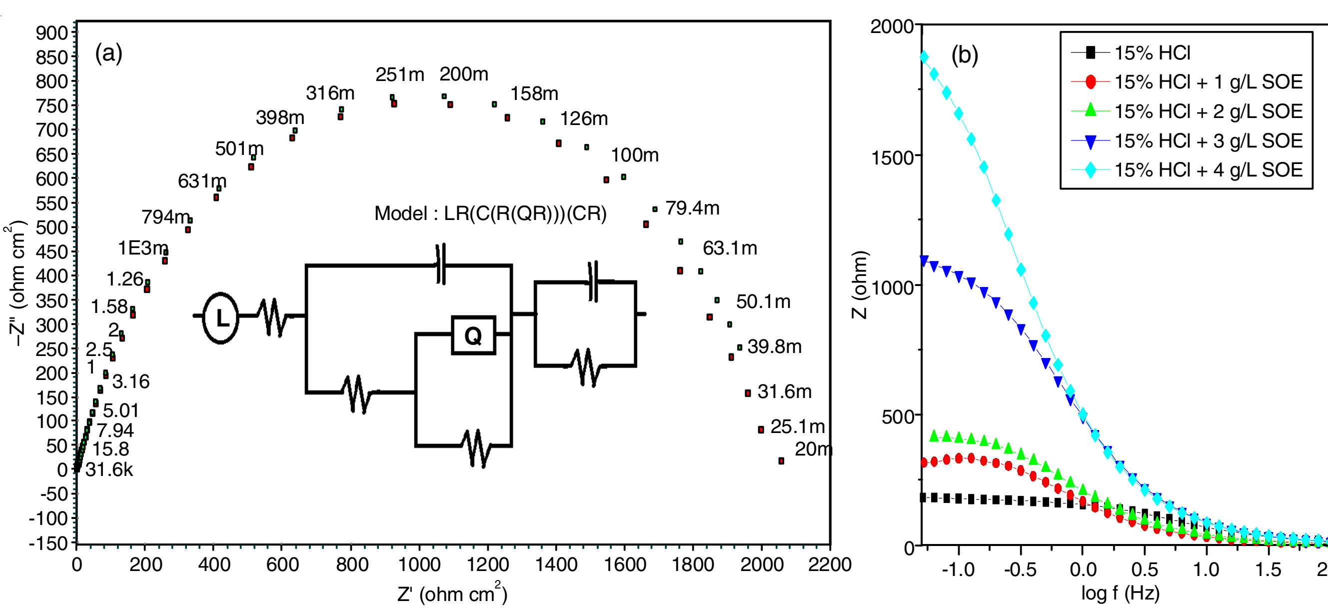

Fig. 3. (a) Impedance data curve fitting with equivalent circuit. (b) Bode-Z plots for SS-410 in 15% HCl solution without and with different concentrations of *S. officinarum* extract (SOE)

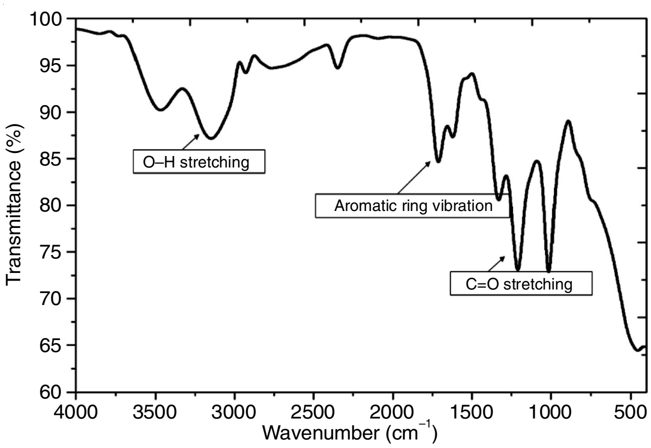

Fig. 4. FT-IR spectra of *S. officinarum* extract (SOE)

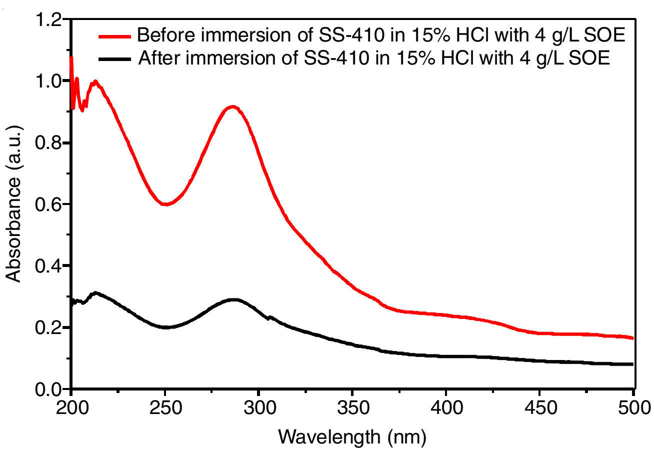

Fig. 5. UV-visible spectra of the *S. officinarum* extract (SOE) after and before immersion of SS-410 for 24 h at 298 K

solution and steel sample immersed in 15% HCl solution with 4 g/L *S. officinarum* extract, respectively. It is clear from the SEM morphology that the SS-410 sample immersed in 15% HCl solution has rough and corroded surface while the surface of SS-410 sample immersed in 15% HCl solution with 4 g/L *S. officinarum* extract appeared smooth due to corrosion inhibition activity of the *S. officinarum* extract [26,27].

AFM study: The AFM images of abraded, SS-410 immersed in HCl containing acidic media and immersed in acidic media with 4 g/L *S. officinarum* extract solution are shown in Fig. 6d, e and f, respectively. The surface roughness value for abraded steel sample and steel sample immersed in 15% HCl solution were 24.52 nm and 921.15nm, respectively. Increase in the surface roughness after immersion in HCl without *S. officinarum* extract as corrosion inhibitor indicated the level of corrosion as the abraded SS-410 samples surface loses smoothness as a result of corrosion [28,29]. The SS-410 samples immersed in HCl containing 4g/L *S. officinarum* extract possessed comparatively lower 212.263 nm surface roughness as a result of corrosion inhibitory activity of phytochemicals present in *S. officinarum* extract.

XRD study: The XRD spectra were obtained in three different conditions: (i) polished stainless steel immersed, (ii) SS-410 immersed in 15% HCl solution and (iii) for SS-410 immersed in 15% HCl solution with 4 g/L *S. officinarum* extract. As from Fig. 7, it is clear that the intensity of iron oxide peak in between 40º.The iron oxide peaks in SS-410 immersed in corrosive media is disappeared when SS-410 immersed in the corrosive media containing *S. officinarum* extract [30].

Theoretical studies: The frontier molecular orbital density distributions (LUMO and HOMO) with optimum structures

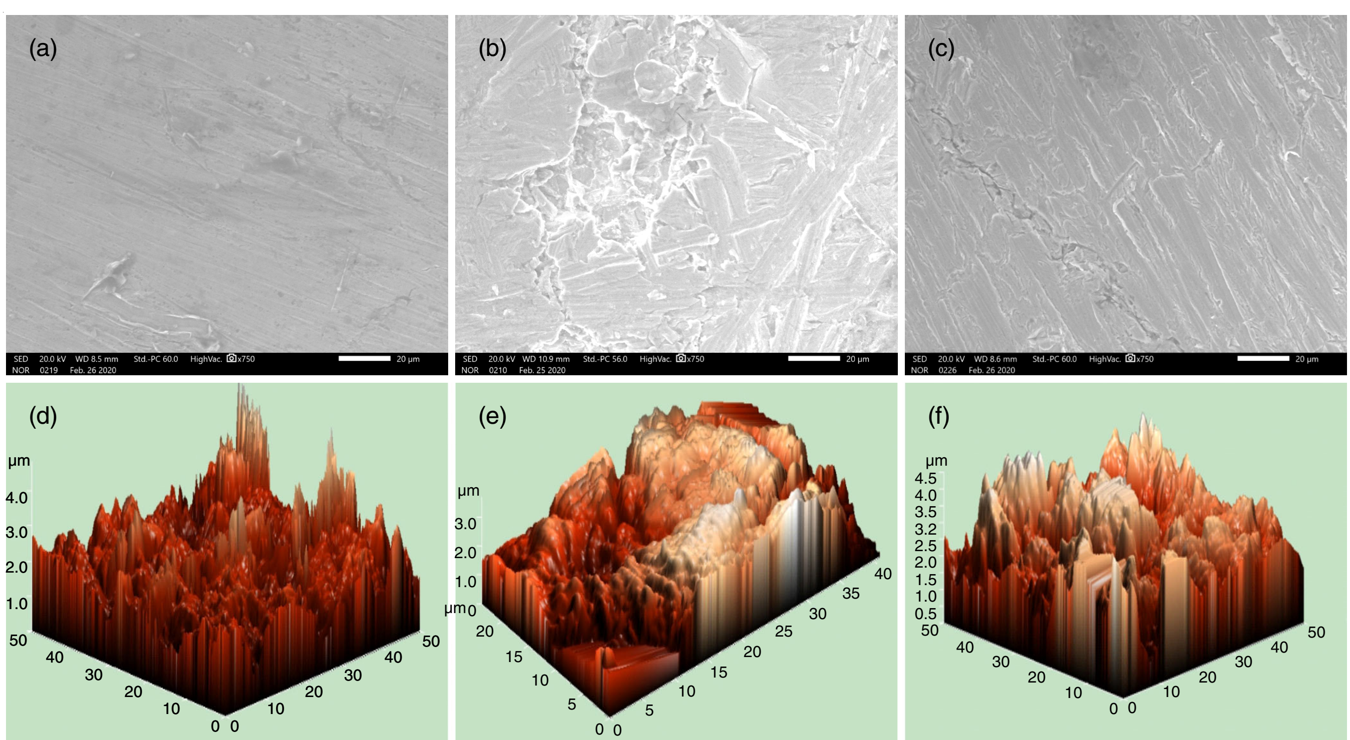

Fig. 6. (a,d) Images of SEM, AFM for abraded SS-410, (b,e) Images of SEM, AFM for SS-410 immersed in 15% HCl solution, (c,f) Images of SEM, AFM for SS-410 immersed in 15% HCl solution with 4 g/L *S. officinarum* extract (SOE)

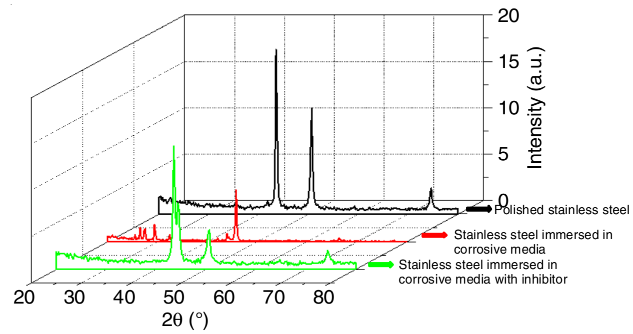

Fig. 7. XRD spectra of 4 g/L *S. officinarum* extract (SOE) on the surface of SS-410

of phytochemicals presents in *S. officinarum* extract are shown in Fig. 8. The key parameters of quantum chemical calculations are the energy of highest occupied molecular orbital (E_{HOMO}), energy of lowest unoccupied molecular orbital (E_{LUMO}), ΔE (energy gap between LUMO and HOMO), back donation energy ($\Delta E_{back\ donation}$), global hardness (σ) and softness (η) [31-33]. These parameters were calculated with the help of following eqns. 7-10:

$$\Delta E = E_{LUMO} - E_{HOMO} \quad (7)$$

$$\eta = \frac{1}{2}(E_{LUMO} - E_{HOMO}) \quad (8)$$

$$\sigma = \frac{1}{\eta} \quad (9)$$

$$\Delta E_{Back\ donation} = -\frac{\eta}{4} \quad (10)$$

The phytochemicals of *S. officinarum* extract interacts with the steel surface to make the parameters of theoretical study changes as found clearly from the data in Table-4. The energy gap of molecular orbital follows the order:luteolin > chromogenic acid > *p*-hydroxybenzoic acid > cinnamic acid > sawamilletin, which indicates the order of donation of electrons to the vacant *d*-orbital of iron. Luteolin has the lowest ΔE (5.97 eV), which shows the good stability of Fe-luteolin complex. The higher value of $\Delta E_{back\ donation}$ of luteolin shows the higher stability of Fe-luteolin complex. Hence, the inhibition effect follows the order: luteolin > chromogenic acid > *p*-hydroxybenzoic acid > cinnamic acid > sawamilletin. So, luteolin can be assumed to be the most essential component in the inhibition performance of the *S. officinarum* extract.

Proposed mechanism of adsorption: The mechanism of corrosion inhibition of SS-410 by *S. officinarum* extract in 15% HCl solution can be explained on the basis of molecular adsorption. There are two possible mechanisms *i.e.* (i) interactions of donor-acceptor between the π-electrons of *S.*

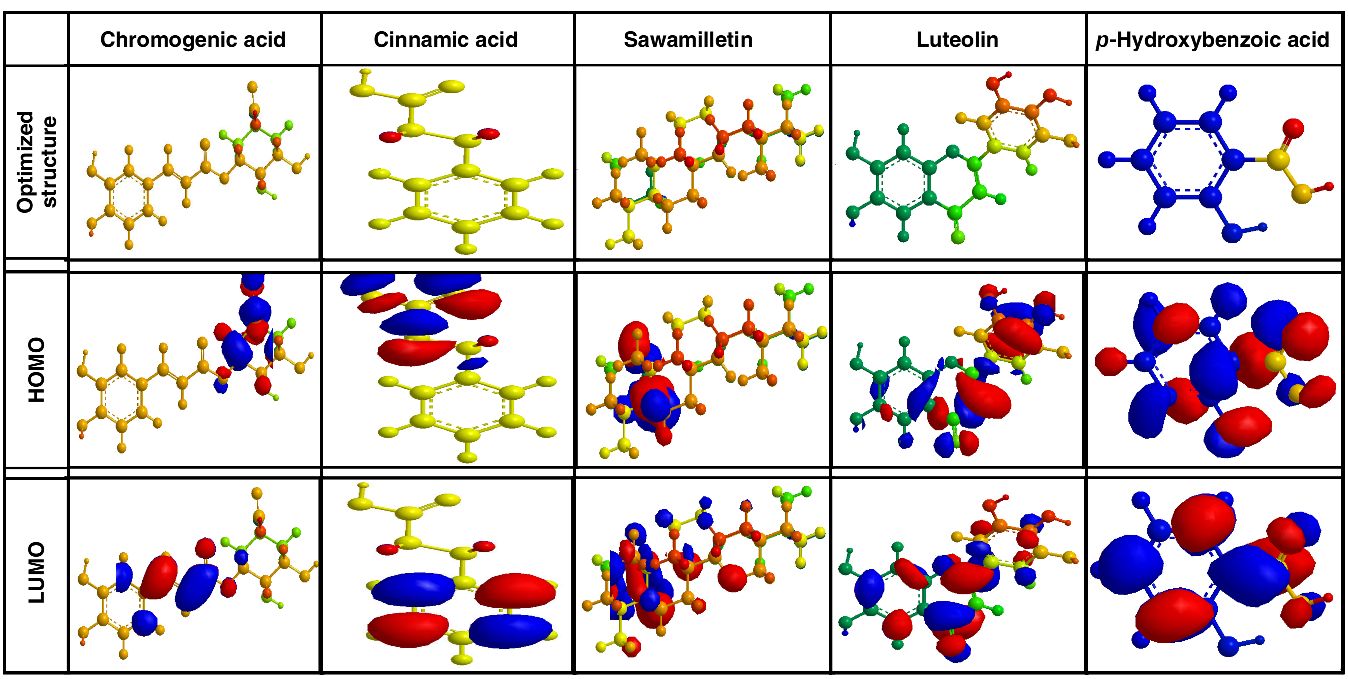

Fig. 8. Optimized structures and frontier molecular orbital density distributions (HOMO & LUMO) obtained by the DFT/B3LYP/6-31G+(d,p) method of phytochemicals present in *S. officinarum* extract (SOE)

TABLE-4
CALCULATED QUANTUM CHEMICAL PARAMETERS OF PHYTOCHEMICALS OF SOE ANALOGUE OBTAINED FROM THE DFT/B3LYP/6-31G+(d,p) METHOD IN THE GAS PHASE

Phytochemicals	E_{HOMO} (eV)	E_{LUMO} (eV)	ΔE (eV)	η (eV)	σ (eV^{-1})	$\Delta E_{B.D}$ (eV)
Chromogenic acid	-10.97	-4.71	6.27	3.13	0.31	-0.78
Cinnamic acid	-12.56	-1.70	10.86	5.43	0.18	-1.35
Sawamilletin	-1.66	21.85	23.51	11.75	0.08	-2.75
Luteolin	-10.01	-4.04	5.97	2.98	0.33	-0.74
p-Hydroxybenzoic acid	-12.45	-3.65	8.80	4.40	0.22	-1.10

officinarum extract and empty *d*-orbitals of SS-410 surface, and/or (ii) interaction between electrons of heteroatoms in inhibitor and vacant *d*-orbital of SS-410 as shown in Fig. 9.

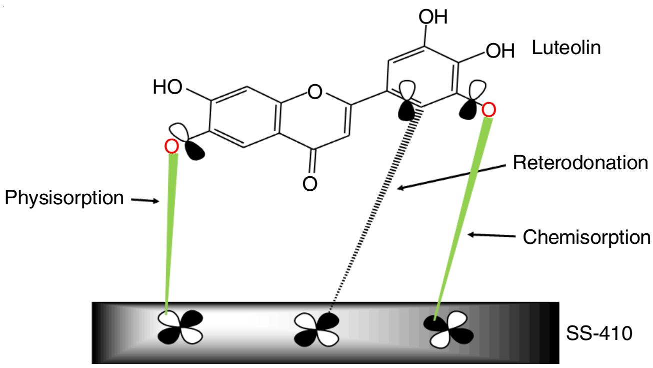

Fig. 9. Schematic representation of the adsorption behaviour of the key phytochemical, salicin molecule on the surface of SS-410

Conclusion

The *S. officinarum* extract has anticorrosive activity for SS-410 in 15% HCl solutions. The mixed type of inhibition is proved by potentiodynamic polarization and has the maximum inhibition efficiency of 90.21% at 4 g/L. The surface morphological studies confirmed the adsorption of SOE on the steel surface. The adsorption of *S. officinarum* extract on SS-410 followed Langmuir adsorption isotherm. Theoretical quantum chemical calculations revealed that the energy of frontier molecular orbital of phytochemicals present in *S. officinarum* extract are well proportioned. Such structures are difficult to form chemical bond active centers, which support the negative sign of the E_{HOMO} values.

ACKNOWLEDGEMENTS

The authors are thankful to Central Instrumental Facility, Lovely Professional University for providing the electrochemical instrument facilities.

CONFLICT OF INTEREST

The authors declare that there is no conflict of interests regarding the publication of this article.

REFERENCES

1. G. Koch, Cost of Corrosion, Trends in Oil and Gas Corrosion Research and Technologies, pp. 3-30 (2017).
2. G.Q. Liu, Z.Y. Zhu, W. Ke, E.H. Han and C.L. Zeng, *Corrosion*, **57**, 730 (2001); https://doi.org/10.5006/1.3290401
3. N. Haghdadi, M. Laleh, M. Moyle and S. Primig, *J. Mater. Sci.*, **56**, 64 (2021); https://doi.org/10.1007/s10853-020-05109-0
4. W.W. Nik, F. Zulkifli, O. Sulaiman, K.B. Samo and R. Rosliza, *IOP Conf. Series Mater. Sci. Eng.*, **36**, 012043 (2012); https://doi.org/10.1088/1757-899X/36/1/012043
5. N. Bhardwaj, P. Sharma and V. Kumar, *Corros. Rev.*, **39**, 27 (2021); https://doi.org/10.1515/corrrev-2020-0046
6. P.D. Krell, S. Li and H. Cong, *Corros. Sci.*, **122**, 41 (2017); https://doi.org/10.1016/j.corsci.2017.03.027
7. M.A. Quraishi and R. Sardar, *Corrosion*, **58**, 748 (2002); https://doi.org/10.5006/1.3277657
8. M. Yadav, U. Sharma and P.N. Yadav, *Egypt. J. Petroleum*, **22**, 335 (2013); https://doi.org/10.1016/j.ejpe.2013.10.001
9. F. Bentiss, M. Lebrini, M. Lagrenee, M. Traisnel, A. Elfarouk and H. Vezin, *Electrochim. Acta*, **52**, 6865 (2007); https://doi.org/10.1016/j.electacta.2007.04.111
10. K.F. Khaled, *Appl. Surf. Sci.*, **252**, 4120 (2006); https://doi.org/10.1016/j.apsusc.2005.06.016
11. A.A. Ganash, *Materials*, **12**, 3013 (2019); https://doi.org/10.3390/ma12183013
12. A. El Bribri, M. Tabyaoui, B. Tabyaoui, H. El Attari and F. Bentiss, *Mater. Chem. Phys.*, **141**, 240 (2013); https://doi.org/10.1016/j.matchemphys.2013.05.006
13. N.A. Odewunmi, S.A. Umoren and Z.M. Gasem, *J. Ind. Eng. Chem.*, **21**, 239 (2015); https://doi.org/10.1016/j.jiec.2014.02.030
14. M.P. Chakravarthy and K.N. Mohana, *Int. Sch. Res. Notices*, **2014**, 687276 (2014); https://doi.org/10.1155/2014/687276
15. N. Soltani, N. Tavakkoli, M. Khayat Kashani, A. Mosavizadeh, E.E. Oguzie and M.R. Jalali, *J. Ind. Eng. Chem.*, **20**, 3217 (2014); https://doi.org/10.1016/j.jiec.2013.12.002
16. F. Zulkifli, N. Ali, M.S.M. Yusof, M.I.N. Isa, A. Yabuki and W.B. Wan Nik, *Prog. Org. Coat.*, **105**, 310 (2017); https://doi.org/10.1016/j.porgcoat.2017.01.017
17. M. Srivastava, P. Tiwari, S.K. Srivastava, R. Prakash and G. Ji, *J. Mol. Liq.*, **236**, 184 (2017); https://doi.org/10.1016/j.molliq.2017.04.017
18. W.B. Wan Nik, H.M. Hajar, M.J. Suriani, M.G.M. Sabri and M.J. Ghazali,, *J. Mech. Eng. Sci.*, **11**, 3179 (2017); https://doi.org/10.15282/jmes.11.4.2017.20.0286
19. N.Z.N. Hashim, E.H. Anouar, K. Kassim, H.M. Zaki, A.I. Alharthi and Z. Embong, *Appl. Surf. Sci.*, **476**, 861 (2019); https://doi.org/10.1016/j.apsusc.2019.01.149
20. A.A. Aksüt, W.J. Lorenz and F. Mansfeld, *Corros. Sci.*, **22**, 611 (1982); https://doi.org/10.1016/0010-938X(82)90042-7
21. R. Idouhli, Y. Koumya, M. Khadiri, A. Aityoub, A. Abouelfida and A. Benyaich, *Int. J. Ind. Chem.*, **10**, 133 (2019); https://doi.org/10.1007/s40090-019-0179-2
22. K.K. Alaneme, S.J. Olusegun and O.T. Adelowo, *Alexandria Eng. J.*, **55**, 673 (2016); https://doi.org/10.1016/j.aej.2015.10.009
23. O.O. Ogunleye, A.O. Arinkoola, O.A. Eletta, O.O. Agbede, Y.A. Osho, A.F. Morakinyo and J.O. Hamed, *Heliyon*, **6**, 3205 (2020); https://doi.org/10.1016/j.heliyon.2020.e03205
24. P.J. Ramakrishnan, V.D.K. Janardhanan, R. Sreekumar and K.P. Mohan, *Int. J. Corros.*, **2014**, 487103 (2014); https://doi.org/10.1155/2014/487103
25. P. Leena, N.H. Zeinul Hukuman, A.R. Biju and M. Jisha, *J. Electrochem. Sci. Technol.*, **10**, 231 (2019); https://doi.org/10.5229/JECST.2019.10.2.231
26. N.A.A. Talib, S. Zakaria, C.C. Hua and N.K. Othman, *AIP Conf. Proc.*, **1614**, 171 (2014); https://doi.org/10.1063/1.4895191
27. Y. Yaocheng, Y. Caihong, A. Singh and Y. Lin, *New J. Chem.*, **43**, 16058 (2019); https://doi.org/10.1039/C9NJ03378E
28. N.K. Gupta, P.G. Joshi, V. Srivastava and M.A. Quraishi, *Int. J. Biol. Macromol.*, **106**, 704 (2018); https://doi.org/10.1016/j.ijbiomac.2017.08.064
29. C. Verma, M.A. Quraishi, E.E. Ebenso and I. Bahadur, *J. Bio-and Tribo-Corrosion*, **4**, 33 (2018); https://doi.org/10.1007/s40735-018-0150-3
30. S. Deng and X. Li, *Corros. Sci.*, **55**, 407 (2012); https://doi.org/10.1016/j.corsci.2011.11.005
31. K.H. Hassan, A.A. Khadom and N.H. Kurshed, *South Afr. J. Chem. Eng.*, **22**, 1 (2016); https://doi.org/10.1016/j.sajce.2016.07.002
32. K.F. Al-Azawi, I.M. Mohammed, S.B. Al-Baghdadi, T.A. Salman, H.A. Issa, A.A. Al-Amiery, T.S. Gaaz and A.A.H. Kadhum, *Results in Physics*, **9**, 278 (2018); https://doi.org/10.1016/j.rinp.2018.02.055
33. Y. Koumya, R. Idouhli, A. Oukhrib, M. Khadiri, A. Abouelfida and A. Benyaich, *Int. J. Electrochem.*, **2020**, 5620530 (2020); https://doi.org/10.1155/2020/5620530